Aquatic Life and Ecosystems
https://www.sciltp.com/journals/ale

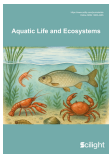

Article

Digestive and Metabolic Functional Responses of Juvenile Yellowfin Tuna (*Thunnus albacares*) to Acute Acidification Stress

Xiaoyan Wang [1,2,3,4,5,†], Xuancheng Liu [6,†], Zhengyi Fu [1,2,3,4,5,6,7], Jing Bai [8] and Zhenhua Ma [1,2,3,4,5,7,*]

[1] Key Laboratory of Efficient Utilization and Processing of Marine Fishery Resources of Hainan Province, Sanya Tropical Fisheries Research Institute, Sanya 572018, China
[2] South China Sea Fisheries Research Institute, Chinese Academy of Fishery Sciences, Guangzhou 510300, China
[3] Hainan Engineering Research Center for Deep-Sea Aquaculture and Processing, Sanya 572018, China
[4] International Joint Research Center for Conservation and Application of Fishery Resources in the South China Sea, Sanya 572018, China
[5] Hainan Fisheries Innovation Research Institute, Chinese Academy of Fishery Sciences, Sanya 572024, China
[6] College of Life Science and Food, Inner Mongolia Minzu University, Tongliao 028000, China
[7] College of Science and Engineering, Flinders University, Adelaide, SA 5001, Australia
[8] Hainan Shuancheng Marine Technology Development Co., Ltd., Haikou 570100, China
* Correspondence: zhenhua.ma@scsfri.ac.cn
† These authors contributed equally to this work.

How To Cite: Wang, X.; Liu, X.; Fu, Z.; et al. Digestive and Metabolic Functional Responses of Juvenile Yellowfin Tuna (*Thunnus albacares*) to Acute Acidification Stress. *Aquatic Life and Ecosystems* **2025**. https://doi.org/10.53941/ale.2025.100004

Received: 21 August 2025
Revised: 4 September 2025
Accepted: 8 September 2025
Published: 11 September 2025

Abstract: This study investigated the tolerance of juvenile yellowfin tuna (*Thunnus albacares*) to acute acidification by determining the activities of trypsin, pepsin, α-amylase (AMS), lipase (LPS), lactate dehydrogenase (LDH), pyruvate kinase (PK), and Na^+K^+-ATPase (NKA) under varying pH conditions, combined with histological section preparation to examine morphological changes. The research aims to provide fundamental reference data for the cage aquaculture of this species. The main findings were as follows: Protease activity increased at pH 7.6; α-amylase activity elevated in the pyloric caeca and liver at pH 7.1, while both α-amylase and lipase activities increased in the stomach at pH 6.6. Foregut enzyme activities decreased with increasing acidity. Hepatic alanine aminotransferase and aspartate aminotransferase were significantly elevated at pH 7.6, whereas gill metabolic enzymes peaked at pH 6.6. Histological analyses showed shortened bends in the midgut villi visible to the naked eye and gill lamellae hyperplasia under low pH conditions. These results indicate moderate adaptability at pH 7.6 but marked physiological stress at pH 6.6.

Keywords: environment; pH; histomorphology; marine organisms

1. Introduction

The aquatic environment is the habitat for aquatic animals to survive [1], and pH is one of the important factors in which subtle changes may affect the growth, reproduction, metabolism and survival of most aquatic organisms [2,3]. The causes and types of changes in water body pH are complex. According to the Intergovernmental Panel on Climate Change (IPCC), human activities have increased atmospheric carbon dioxide concentrations by 47% since before the Industrial Revolution [4]. Human activities in densely populated estuarine and coastal regions can have a significant effect on the aquatic environment, potentially leading to sudden disturbances that cause a rapid, short-term drop in seawater pH [5–7]. These changes in the aquatic environment suggest that changes in seawater acidity are

more unpredictable than one might think, posing significant risks to ecosystems and their wide range of organisms that depend on the stability of the chemical environment of the water column.

Typically, the optimal pH range helps fish achieve optimal metabolic efficiency, while deviation from this range triggers a series of chain reactions. A decrease in pH leads to the accumulation of CO_2 in the blood (hypercapnia), forcing fish to maintain acid-base balance through ion regulation (e.g., increasing HCO_3^- accumulation and excreting H^+). This process consumes energy, diverting resources needed for growth and reproduction [8,9]. For example, Atlantic cod (*Gadus morhua*) under pH 7.7 conditions experience a 30% increase in ion regulatory energy expenditure, resulting in a 15% reduction in growth rate [10]. Antarctic fish (Notothenia rossi) at pH 7.6 exhibit impaired mitochondrial function, with aerobic metabolic capacity decreasing by 20% [11]. When pH < 7.8, fish may also display "metabolic suppression"—reducing basal metabolic rate to conserve energy, but at the cost of diminished locomotion, feeding, and immune function [12]. For instance, European seabass (*Dicentrarchus labrax*) at pH 7.6 shows a 25% reduction in digestive enzyme activity and decreased food conversion efficiency [13]. It has also been shown that low pH environments lead to a slowing down of shellfish metabolism [14] and a significant decrease in the activity of digestive enzymes such as α-amylase and lipase [15,16]. Additionally, low pH environments cause fish to increase energy expenditure during resting states (non-active, non-digestive, and non-stressed conditions) to maintain basic physiological functions such as respiration, ion regulation, and cellular repair. This is accompanied by enhanced acid-base regulation (Na^+K^+-ATPase activity) [17], gill deformation and severe contraction [18], chlorocyte hypertrophy and hyperplasia [19], and intestinal mucosal damage accompanied by accelerated intestinal cell turnover [20], resulting in organ damage in two temperate commercially important fish species—Atlantic cod and herring [21,22]. Invertebrates are more sensitive to environmental changes, so most studies on water acidification have focused on mollusks or echinoderms. This has led to a lack of understanding regarding the responses of fish, particularly those of greater commercial value. Throughout the Pacific Ocean, the main habitat for juvenile yellowfin tuna (*Thunnus albacares*) is in the 0–50 m mixed layer, where seawater pH ranges from 7.80 to 8.1 [23], but in some regional upwelling areas (e.g., the eastern Pacific Ocean), ocean mixing can lead to a further decrease in pH in the surface layer [24,25]. Research has shown that juvenile yellowfin tuna reared under low pH conditions of 7.6 for one week exhibit damage to organs including the kidneys, pancreas, eyes, and muscles. Liver tissue deteriorates, with features such as darkened and indistinct cell nuclei and increased lipid deposition [26]. Furthermore, it is anticipated that both survival rates and growth of the juveniles will decline in the near future [27].

Tuna is a popular fish for the commercial fishing industry as it is favoured by consumers due to its fast growth rate and high content of crude protein and unsaturated fatty acids [28,29]. It has also been shown that tuna stock abundance supports the sustainable development of industries such as coral reefs, coastal fisheries and mariculture, and is vital to the ecosystem [30]. However, due to chronic overfishing, the World Conservation Union (IUCN) has listed yellowfin tuna as Near Threatened [31]. Yellowfin tuna in the Pacific is currently nearly fully exploited and there is uncertainty about recent and future replenishment and biomass levels [32]. Compared to other tuna species, yellowfin tuna exhibit a broader distribution across tropical and subtropical waters. Their rapid juvenile growth rate makes them well-suited for aquaculture in coastal areas with warmer surface temperatures, factors that have propelled them to prominence as a popular aquaculture species [33]. The Deepwater Aquaculture Technology and Species Development Innovation Team at the Chinese Academy of Fisheries Sciences (CAFS) has successfully introduced offshore deepwater net-pen aquaculture for yellowfin tuna near Lingshui Lizu Autonomous County. A relatively mature and reliable set of procedures has been established for yellowfin tuna harvesting, transportation, feeding, and related techniques [34]. However, comprehensive research on how changes in the seawater environment, particularly in acidity, affect the growth of juvenile yellowfin tuna remains insufficient. The pyloric caeca, stomach, and foregut are the primary digestive organs, while the liver serves as the metabolic hub, with ALT and AST reflecting protein metabolism. The gills, as the frontline organs in contact with the aquatic environment, are responsible for respiration and ion regulation. Due to their high energy demand (relying on glycolysis and Na^+K^+-ATPase to maintain osmotic balance), they, along with the liver, represent systemic metabolism and localized energy regulation, respectively, demonstrating clear physiological specialization. The midgut is the main site for nutrient absorption (proteins, fats, and carbohydrates), and its morphological changes are directly linked to digestive enzyme activity (e.g., protease, lipase, and amylase). In response to the potential challenges posed by ocean acidification to fishery resources, this study focuses on key tissues—pyloric caeca, stomach, foregut, liver, gills, and midgut—employing enzyme activity assays and histological observation. The findings provide critical physiological parameters for tuna cage farming, supporting optimized aquaculture management strategies, improved farming efficiency, and scientific guidance for the sustainable development of marine fisheries.

2. Materials and Methods

2.1. Acute Exposure Experiment

In June 2023, juvenile wild yellowfin tuna were captured by the South China Sea Fisheries Research Institute of the Chinese Academy of Fisheries Sciences near Xincun Harbor in the South China Sea. A total of 72 healthy juveniles, of similar size, were selected (18°22′31.9″ N, 109°58′28.9″ E), with an average body length of 18.21 ± 1.09 cm and a mean weight of 307.49 ± 49.38 g. Juvenile tuna were first temporarily reared in a workshop in the Tropical Aquatic Research and Development Centre for 7 d. During this period, chilled omnivorous fish were fed once a day (at a rate of 5% of the juvenile's body weight). One week later, they were subjected to 48 h of acidification stress in circular tempered drums (5000 L). The experimental seawater used was natural seawater treated with sand filtration. Throughout both the temporary rearing period in the workshop and the formal experimental phase, water quality parameters were maintained consistently: water temperature 22.5 ± 1 °C, DO > 7.5 mg·L^{-1}, $NaNO_2$ < 0.05 mg·L^{-1} and NH_3^-N < 0.05 mg·L^{-1}. Juvenile fish were no longer fed during the experiment. A total of four groups were set up, with natural seawater pH 8.1 [35] as the control group, and with reference to the 'near-term' projection for the year 2100, the 'long-term' projection for the year 2300, and the projected pH levels in the next 300 years, the experimental groups were set to have pH values of 7.6, 7.1, and 6.6 [23,36,37]. Each group consisted of three replicates, with six fish per replicate. The light-dark cycle was set to 12 h each. Seawater pH was regulated using sodium hydroxide (NaOH) solution at mmol·L^{-1} concentrations or 1.0 mmol·L^{-1} hydrochloric acid (HCl) solution [16,38–40]. A pH analyzer (Shenzhen Jingxin Microelectronics Co., Shenzhen, China) was used to measure the seawater's acidity, with corrections made every 2 h to maintain the pH within a ± 0.1 range.

2.2. Anatomical Process

At the conclusion of the experiment, fish were anesthetized using eugenol (50 ppm). Anesthesia was deemed successful when gill cover movement ceased and the fish exhibited no discernible response to touch. Six juvenile fish were selected from each tank. Measure body length using calipers (accurate to 0.01 cm) and record body weight (accurate to 0.01 g). Dissect fish on ice trays using autoclaved instruments according to the method described by Rosseland et al. [41].

Tissues were quickly collected, rinsed in ice-cold physiological saline (0.9%) and excess water was blotted out with filter paper. The foregut and midgut were distinguished following the methodology described by Gonçalves et al. [42]. Place the pyloric caecum, liver, gills, stomach, and foregut into a 2-milliliter cryovial that has been pre-chilled, then rapidly freeze it in liquid nitrogen. After sampling, transfer samples from liquid nitrogen to a −80 °C freezer and complete enzyme activity assays within one week. Remove gills and midgut, fix them in 4% paraformaldehyde (BL 539A, Biosharp Co., Hefei, China) for preservation, and prepare tissue sections.

2.3. Biochemical Analysis

The samples were thawed at 4 °C for 100 min [43] before precise weighing of 0.1–0.2 g tissue specimens. A 9-fold volume of pre-chilled homogenization buffer was added to each sample. The mixture was then mechanically homogenized in an ice-water bath, followed by centrifugation at 3000 rpm for 10 min using a refrigerated high-speed centrifuge. The resulting supernatant was collected for subsequent analytical determinations. To standardize the enzyme activity index across various tissues, the total protein (TP) content in the tissue supernatant is measured.

Total protein (TP, reagent serial number A045-4-2) content was determined by BCA (bicinchoninic acid) (minimum detection limit: 0.5 μg/mL). Under alkaline conditions, proteins reduce Cu^{2+} to Cu^{+}. These Cu^{+} ions form a purple complex with the BCA reagent, are incubated at 37 °C, and the absorbance is measured at 562 nm. As the absorbance is directly proportional to concentration, the protein concentration can be determined by measuring the absorbance. The calculation formula is as follows:

$$Cpr\ (\mu g/mL) = \frac{A_{test} - A_{blank}}{A_{standard} - A_{blank}} * C_{standard} * N$$

In the formula: $A_{Standard}$: Standard concentration 524 μg/mL; *N*: Dilution factor of the sample before testing.

Trypsin activity (Reagent serial number A080-2-1) was determined by the Arginine Ester Hydrolysis Method (minimum detection limit: 10 μg/mL). The enzyme can catalyze the hydrolysis of the ester bond in the substrate arginine ethyl ester. After incubation in a water bath at 37 °C, the absorbance at 253 nm increases, and the enzyme activity can be calculated based on the change in absorbance. The calculation formula is as follows:

$$Trypsin\ Activity\ (\mu/mgprot) = \frac{A_{sample} - A_{blank}}{0.003} * \frac{V_{reaction}}{V_{sample}} \div T \div (Cpr * V_{sample})$$

In the formula: $V_{reaction}$: Total reaction system volume 1.5 + a (mL); V_{sample}: Sample volume a (mL); *T*: Reaction time 20 min; *Cpr*: Protein concentration of the homogenate sample (mgprot/mL, where "prot" refers to protein).

Pepsin activity (Reagent serial number A080-1-1) was determined by Folin-Ciocalteu reagent method (minimum detection limit: 0.15 μ/mL). This method involves incubation at 37 °C, during which pepsin hydrolyzes proteins to generate phenolic amino acids. The phenol reagent can be reduced by these phenolic amino acids to form a blue-colored complex. The absorbance is then measured colorimetrically at 660 nm. The calculation formula is as follows:

$$Pepsin\ Activity\ (\mu/mgprot) = \frac{A_{sample} - A_{control}}{A_{standard} - A_{blank}} * C_{standard} \div T * \frac{V_{reaction}}{V_{sample}} \div Cpr$$

In the formula: $C_{Standard}$: Standard concentration 50 μg/mL; *T*: Reaction time 10 min; $V_{reaction}$: Total reaction volume 0.64 mL; V_{sample}: Sample volume 0.04 mL; *Cpr*: Protein concentration of tissue homogenate (mg prot × mL^{-1}, where "prot" refers to protein).

α-Amylase (AMS, reagent serial number C016-1-2) activity was determined by the iodometric method (minimum detection limit: 0.01 μ/mgprot). The enzyme catalyzes the hydrolysis of starch into glucose, maltose, and dextrin. When the substrate concentration is known and in excess, the mixture is incubated in a water bath at 37 °C. After adding iodine solution, a blue complex forms with the unhydrolyzed starch. The absorbance is measured at 660 nm. The calculation formula is as follows:

$$AMS\ Activity\ (\mu/mgprot) = \frac{A_{blank} - A_{test}}{A_{blank}} * \frac{0.4 * 0.5}{10} * \frac{30min}{7.5min} \div (A_{sample} * C)$$

In the formula: A_{sample}: Sample volume 0.1 mL; *C*: Protein concentration of the sample to be tested (mg prot/mL).

Lipase (LPS, reagent serial number A054-2-1) activity was determined by colourimetric substrate method (lowest limit of detection: 0.06 μ/mL), 1,2-O-Dilauryl-racemic-glycerol + valeric acid-(6-methylthiohalogen) ester, Valeric acid-(6-methylthiobenzyl) ester → Valeric acid + 6-methylthiobenzyl (colour development. The activity of lipase is determined by measuring the formation rate of the red product methylresorufin at 580 nm after incubation at 37 °C. The calculation formula is as follows:

$$LPS\ Activity\ (\mu/gprot) = \frac{A_{\boldsymbol{sample}} - A_{blank}}{A_{\boldsymbol{standard}} - A_{blank}} * C_{standard} \div Cpr$$

In the formula: $C_{standard}$: Standard concentration (μ/L); *Cpr*: Homogenate protein concentration (g prot/L, where "prot" = protein).

The activity of Na^+K^+-ATPase (NKA, reagent catalog number A070-5-1) was assessed through a colorimetric method that quantifies inorganic phosphate, with a detection sensitivity of 0.0026 μmol/mL. ATPase can decompose ATP to produce ADP and inorganic phosphorus. The activity of ATPase can be determined by measuring the inorganic phosphorus content. After incubation at 37 °C, the absorbance is read at 636 nm. The calculation formula is as follows:

$$NKA\ Activity\ (\mu/gprot) = \frac{A_{test} - A_{control}}{A_{\boldsymbol{standard}} - A_{blank}} * C_{standard} * \frac{60}{T} * N \div Cpr$$

In the formula: $C_{standard}$: Phosphorus standard concentration, 0.02 μmol/mL; *T*: Enzymatic reaction time = 10 min; *N*: Dilution factor of enzymatic reaction system, 7.8 (0.78 mL/0.1mL); *Cpr*: Tissue homogenate protein concentration, mgprot/mL (prot refers to protein).

Lactate dehydrogenase (LDH, reagent serial number A020-2-2) activity was determined by LDH release assay (minimum detection limit: 1 μ/L). Under the catalysis of LDH, lactate is converted to pyruvate. The generated pyruvate further reacts with 2,4-dinitrophenylhydrazine under alkaline conditions at 37 °C to form a reddish-brown product, pyruvic acid dinitrophenylhydrazone. According to Beer-Lambert's Law, the activity of lactate dehydrogenase can be quantitatively determined by measuring the absorbance of this reddish-brown product (pyruvic acid dinitrophenylhydrazone) at 440 nm. The calculation formula is as follows:

$$LDH\ Activity\ (\mu/gprot) = \frac{A_{\boldsymbol{test}} - A_{control}}{A_{\boldsymbol{standard}} - A_{blank}} * C_{standard} \div Cpr$$

In the formula: $C_{standard}$: Standard solution concentration, 0.2 μmol/mL; *Cpr*: Sample protein concentration, g prot/mL (prot refers to protein).

Pyruvate kinase (PK, reagent serial number A076-1-1) activity was determined by Pyruvate Kinase Activity Assay (minimum detection limit: 1.3 μ/L). In the presence of ADP, it catalyzes the conversion of PEP to pyruvate. The pyruvate is then converted to lactate by LDH, accompanied by the oxidation of NADH to NAD. The reaction

mixture is incubated in a water bath at 37 °C, and the absorbance is measured at 340 nm. The calculation formula is as follows:

$$PK\ Activity\ (\mu/gprot) = \frac{\Delta A}{6.22 * T * d} * \frac{V_{reaction}}{V_{sample}} \div Cpr$$

In the formula: 6.22: PEP millimolar extinction coefficient; *T*: Reaction time, 15 min; *d*: Optical path length, 0.5 cm; $V_{reaction}$: Total reaction volume, 1.195 mL; V_{sample}:Sample volume, 0.02 mL; *Cpr*: Tissue homogenate protein concentration, g prot/mL (prot refers to protein).

Alanine aminotransferase (ALT, reagent serial number C009-2-1) and aspartate aminotransferase (AST, reagent serial number C010-2-1) activities were determined by Reitman-Frankel assay (minimum detection limit: μ/L). ALT acts on a substrate composed of alanine and α-ketoglutarate at 37 °C and pH 7.4, producing pyruvate and glutamate. After 30 min (fixed time), 2,4-dinitrophenylhydrazine (DNPH) hydrochloride solution is added to terminate the reaction. Simultaneously, DNPH reacts with the carbonyl group in the ketone acid to form pyruvate hydrazone. The phenylhydrazine forms a red-brown colour under alkaline conditions. The absorbance is measured at 505 nm, and enzyme activity is calculated. AST transfers the amino and ketone groups from α-ketoglutarate and aspartate to form glutamate and oxaloacetate. Oxaloacetate can spontaneously decarboxylate to form pyruvate during the reaction. Pyruvate reacts with 2,4-dinitrophenylhydrazine to form 2,4-dinitrophenylhydrazone. After incubation at 37 °C, the product develops a reddish-brown color in alkaline solution. The absorbance is measured at 510 nm, and the enzyme activity units can be determined by referring to the standard curve. The calculation formula is as follows:

$$AST/ALT\ Activity\ (\mu/gprot) = A * 0.482 \div Cpr$$

In the formula: *A*: Obtained from standard curve AST activity (Karmen units); 0.482: Conversion factor from Karmen units to U/L; *Cpr*: Tissue homogenate protein concentration, g prot/L (prot refers to protein).

The above parameters were measured using a hybrid microplate reader (BioTek Instruments, Winooski, USA) and a UV-visible spectrophotometer (Shanghai Meipan Instrument Co., Ltd., Shanghai, China), following the kits provided by Nanjing Jiancheng Bioengineering Research Institute and the manufacturer's guidelines. The procedure was repeated three times for each sample, and negative and positive controls were set for each determination.

2.4. Histological Analysis

Within two weeks after the autopsy, remove the tissue from the paraformaldehyde fixative, dehydrate it, and embed it in paraffin. During embedding, the tissue must be thoroughly flattened at the bottom of the embedding mould to ensure that the expected observation section of the tissue is at the same level. First, a small amount of liquid paraffin is dripped into the embedding box to make the bottom of the moulded wax block smooth and flat, and then the observation surface of the tissue is flattened at the bottom of the embedding box. After the wax block has solidified at 4 °C, it is sectioned into 4 μm-thick slices using a Leica rotary microtome (Leica Microsystems (Shanghai) Co., Ltd., Shanghai, China). The slices are spread in a warm water bath, picked up with a slide, dried in a 37 °C oven, and then stained with hematoxylin and eosin (H & E). Neutral resin is added to the centre of the section for mounting. A cover slip (24 × 50 mm) is slowly tilted over the section to avoid air bubbles, and excess resin is gently pressed out. Excess resin at the edges is removed with tweezers, and the section is placed in a 37 °C constant-temperature incubator for 2 h for permanent preservation. Observation and imaging were performed using a DMI8 fluorescence inverted microscope produced by Leica Microsystems GmbH in Wetzlar, Germany, at 400× magnification. When selecting gill tissue sections, choose those with intact gill filament structures, clearly visible epithelial cells, and mitochondria-rich cells (MRCs), while avoiding the edges of gill arches. For intestinal tissue sections, select longitudinal sections of mucosal folds (avoid oblique cuts that may cause artificial shortening) with clearly visible intestinal villi. To assess tissue damage induced by low pH environments, three fish tissue samples were randomly selected from each treatment group, ten fields of view were randomly chosen for each fish and observed (400×). According to the method described by Huang et al. [44]. A semi-quantitative scoring system was employed to evaluate the degree of tissue damage. Lesions were classified into five grades based on morphological characteristics, ranging from Grade 0 (no lesions) to Grade 4 (severe lesions). Gill scoring criteria encompass four indicators: cellular edema, cellular hyperplasia, cellular adhesion, and cellular necrosis. Midgut scoring criteria include three indicators: villus height, goblet cell, and cytoplasmic vacuolation. Records document the number of damaged cells for each lesion type, with statistical analysis providing quantitative support for histopathological evaluation.

2.5. Data Processing

The experimental data was organized using Excel 2010 software. IBM SPSS Statistics 25.0.was used for statistical analysis, and polynomial regression analysis was performed on the proteases to derive regression equations for calculating the pH values at which the two proteases reached their peaks and the trends in their activity changes. The normality of the data was evaluated using the Shapiro-Wilk test, and homogeneity of variance was assessed using Levene's test. One-way ANOVA followed by the Dunnett test was applied to compare differences between the control and experimental groups. Results were presented as mean ± standard deviation (Mean ± SD), and a p-value of <0.05 was considered statistically significant. Bar graphs were generated using GraphPad Prism 9.5 software.

3. Results

3.1. Effect of Acidification on the Activity of Digestive Enzymes

Under stress conditions, the quadratic coefficients of the regression equations for trypsin and pepsin activities were negative, confirming an inverted U-shaped trend in activity changes. By deriving the regression equations, the second derivative was found to be negative, indicating that both trypsin and pepsin activities peaked at pH 7.6 (Supplementary Materials Tables S1 and S2). The activity of both proteases was significantly higher than that of the control group at pH 7.6 ($p < 0.01$) (Figure 1a,b). The lowest activity of pepsin was observed in the pH 6.6 treatment group, and there was a significant difference compared with the control group ($p < 0.05$) (Figure 1b); the lowest activity of trypsin was observed at pH 8.1 (Figure 1a).

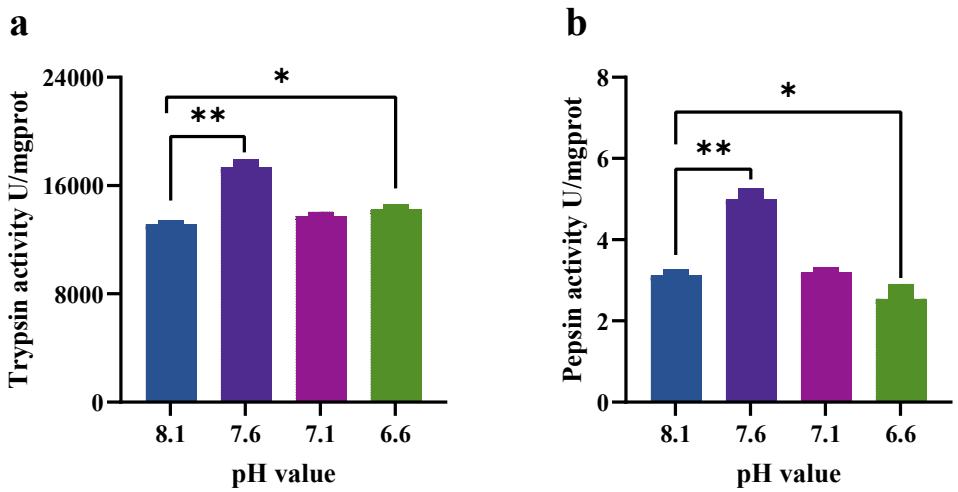

Figure 1. Effects of acute acidification stress on trypsin and pepsin activity (n = 6). (**a**): Trypsin activity in the pyloric ceca; (**b**): Pepsin activity in the stomach. An * above the bars indicates a significant difference between the control and experimental groups ($p < 0.05$), ** indicates a highly significant difference ($p < 0.01$), and no mark indicates a non-significant difference ($p > 0.05$).

As seawater pH decreases, the AMS activity in the pyloric caeca and liver of juvenile fish reaches its maximum at pH 7.1, and there is a highly significant difference compared to the control group ($p < 0.01$) (Figure 2a,c). As seawater pH decreased, stomach AMS activity rapidly increased at pH 6.6, significantly higher than the control group ($p < 0.01$) (Figure 2b). As seawater pH decreased, AMS activity in the foregut showed a decreasing trend, reaching the lowest value at pH 6.6, with a highly significant difference compared to the control group ($p < 0.01$) (Figure 2d).

As seawater pH decreases, the activity of lipase (LPS) in the pyloric caecum and liver of juvenile fish exhibits a similar trend, with both reaching a maximum at pH 7.6 and then gradually decreasing (Figure 3a,c). There were no significant differences in LPS activity between the pH 7.6 treatment group and the control group in both tissues ($p > 0.05$). However, LPS activity in the liver was extremely significantly lower than that in the control group at pH 6.6 ($p < 0.05$) (Figure 3c). LPS activity in the stomach rapidly increased at pH 6.6 and showed a highly significant difference compared to the control group ($p < 0.01$) (Figure 3b). As seawater pH decreased, LPS activity in the foregut showed a decreasing trend, reaching a maximum at pH 7.1 and showing a significant difference compared to the control group ($p < 0.05$).

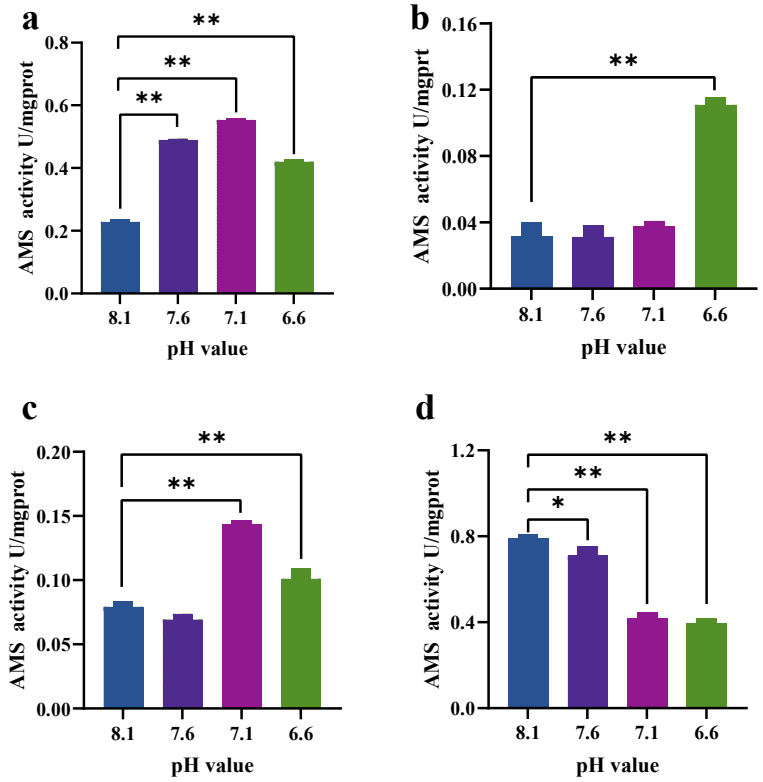

Figure 2. Impact of acute acidification stress on α-amylase (AMS) activity (n = 6). (**a**): pyloric caeca; (**b**): stomage; (**c**): liver; (**d**): foregut. An * above the bars indicates a significant difference between the control and experimental groups ($p < 0.05$), ** indicates a highly significant difference ($p < 0.01$), and no mark indicates a non-significant difference ($p > 0.05$).

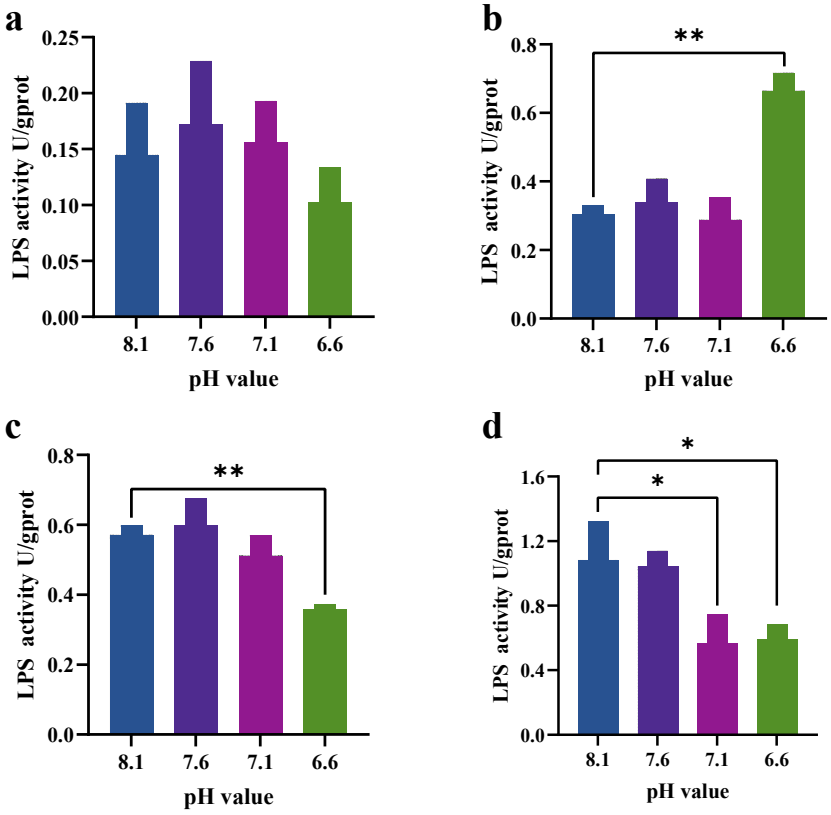

Figure 3. Impact of acute acidification stress on lipase (LPS) activity (n = 6). (**a**): pyloric caeca; (**b**): stomage; (**c**): liver; (**d**): foregut tissue. An * above the bars indicates a significant difference between the control and experimental groups ($p < 0.05$), ** indicates a highly significant difference ($p < 0.01$), and no mark indicates a non-significant difference ($p > 0.05$).

3.2. The Effect of Acidity Changes on the Metabolic Enzyme Activity of Juvenile Fish

As seawater pH decreases, the activity of alanine aminotransferase (ALT) and aspartate aminotransferase (AST) in the liver shows a trend of first increasing and then decreasing (Figure 4a,b). ALT and AST reached their maximum values at pH 7.6, showing extremely significant differences compared to the control group ($p < 0.01$); the activity of both enzymes reached their minimum values at pH 6.6, but there were no significant differences compared to the control group ($p > 0.05$).

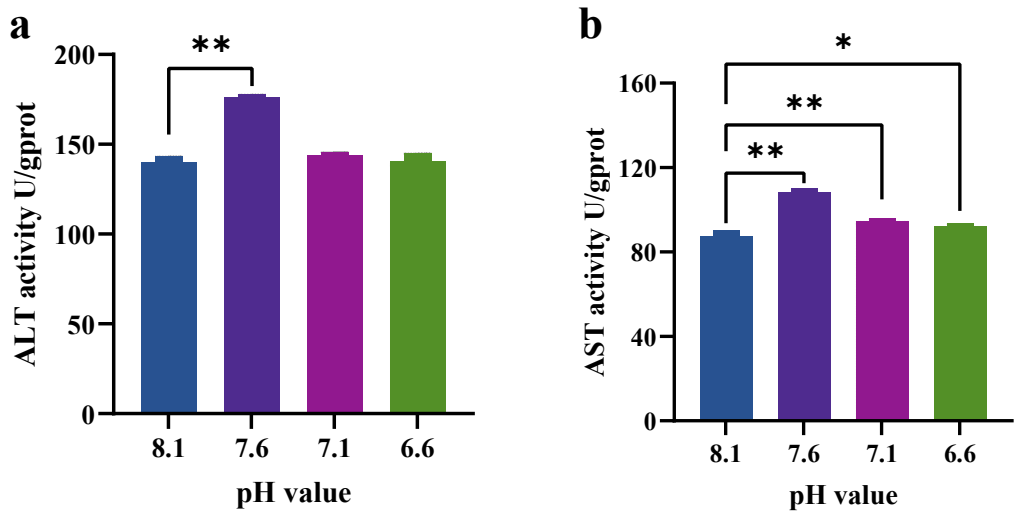

Figure 4. Impact of acute acidification stress on metabolic enzyme activities in the liver (n = 6). a: alanine aminotransferase (ALT) activity; b: aspartate aminotransferase (AST) activity. An * above the bars indicates a significant difference between the control and experimental groups ($p < 0.05$), ** indicates a highly significant difference ($p < 0.01$), and no mark indicates a non-significant difference ($p > 0.05$).

Lactate dehydrogenase (LDH) activity in the gills rapidly increased at pH 6.6, significantly higher than the control group ($p < 0.01$) (Figure 5c). Pyruvate kinase (PK) activity in the gills reached its peak at pH 6.6, significantly higher than the control group ($p < 0.01$) (Figure 5d). As seawater pH decreased, Na^+K^+-ATPase (NKA) activity in the gills showed an increasing trend (Figure 5e), reaching a maximum at pH 6.6, with a significant difference compared to the control group ($p < 0.01$).

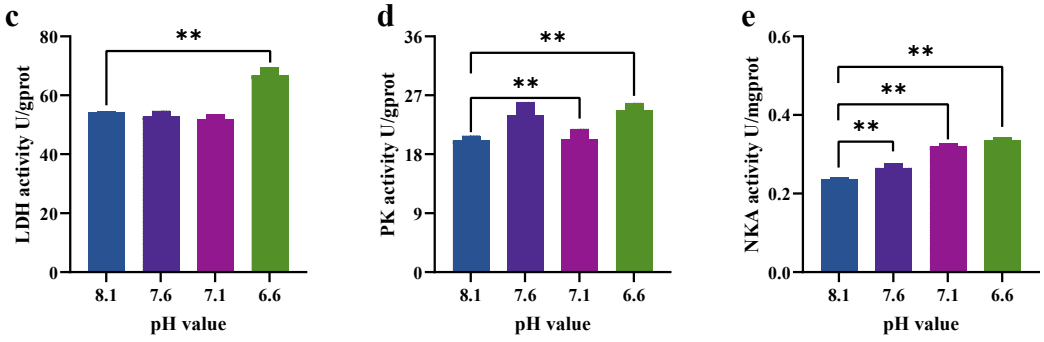

Figure 5. Impact of acute acidification stress on metabolic enzyme activities in the gills (n = 6). (**c**): lactate dehydrogenase (LDH) activity; (**d**): pyruvate kinase (PK) activity; (**e**): Na^+K^+-ATPase (NKA) activity. An * above the bars indicates a significant difference between the control and experimental groups ($p < 0.05$), ** indicates a highly significant difference ($p < 0.01$), and no mark indicates a non-significant difference ($p > 0.05$).

3.3. The Effect of Changes in Acidity on the Histological Structure of the Midgut and Gills

The response of midgut tissue in juvenile yellowfin tuna to acidification stress is shown in Figure 6A–D. In the control group (Figure 6A), the intestinal villi exhibited a ciliated and elongated morphology. As seawater acidity increased, the goblet cells in the midgut displayed characteristics of loose arrangement. In the pH 7.1 treatment group (Figure 6C), the intestinal villi became sparsely distributed with visible curvature. These pathological features were further exacerbated under pH 6.6 conditions (Table 1).

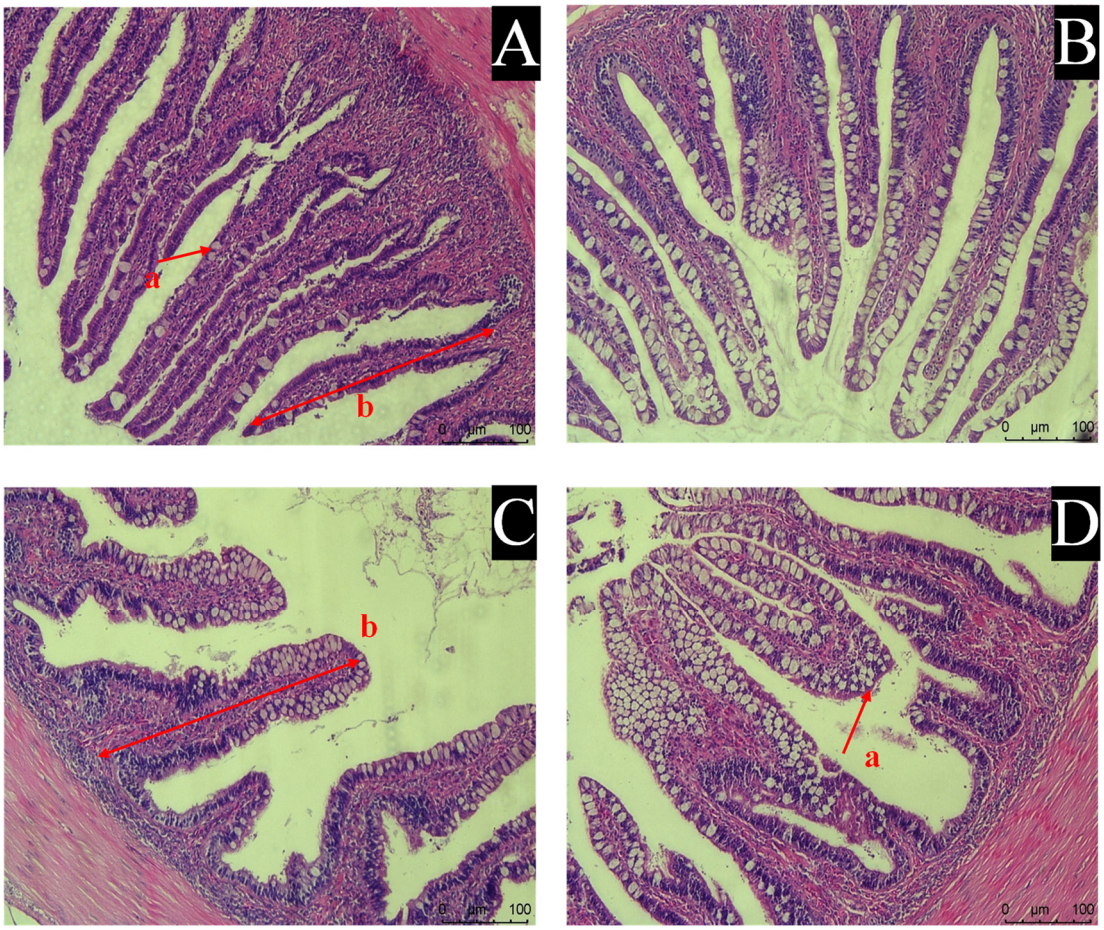

Figure 6. Effect of acute acidification stress on the histological structure of the midgut. (**A**): treatment group with pH 8.1 (control); (**B**): treatment group with pH 7.6; (**C**): treatment group with pH 7.1; and (**D**): treatment group with pH 6.6. a: goblet cells; b: intestinal villi.

Table 1. Semi-quantitative scoring of histopathological damage in the midgut of yellowfin tuna juveniles under different pH treatments.

Group	pH 8.1	pH 7.6	pH 7.1	pH 6.6
villu height	0	0	1	1
goblet cell	0	2	2	3
cytoplasmic vacuolation	0	1	1	2

Note: Three tissue samples were randomly selected from each treatment group, and 10 fields of view were randomly selected from each fish for observation. The severity of lesions was classified according to the number of affected cells per field of view as follows: 0 cells = Grade 0 (normal), 1–5 cells = Grade 1 (mild), 6–10 cells = Grade 2 (moderate), 11–15 cells = Grade 3 (severe), and >15 cells = Grade 4 (highly severe).

Observation of the gills sections revealed that the gill lamellae on both sides of the gill filaments in the control group (Figure 7a) were elongated, well arranged and densely packed with epithelial and columnar cells. Chloride-excreting cells at the base of the gill lamellae were abundant and compactly arranged. In the pH 7.6 treatment group (Figure 7b), slight bulging of lamellar cells was observed together with visible curvature of the gill lamellae. Most lamellae ends were hyperplastic and hypertrophied, and this phenomenon worsened with increasing pH (Table 2). In the pH 6.6 treatment group (Figure 7d), a few adjacent gill lamellae were adherent and fused. The gill lamellae were more curved and irregularly distributed. The gill lamellae displayed pronounced curvature and irregular distribution, while the basal chloride cells became sparsely arranged and developed conspicuous large vacuoles.

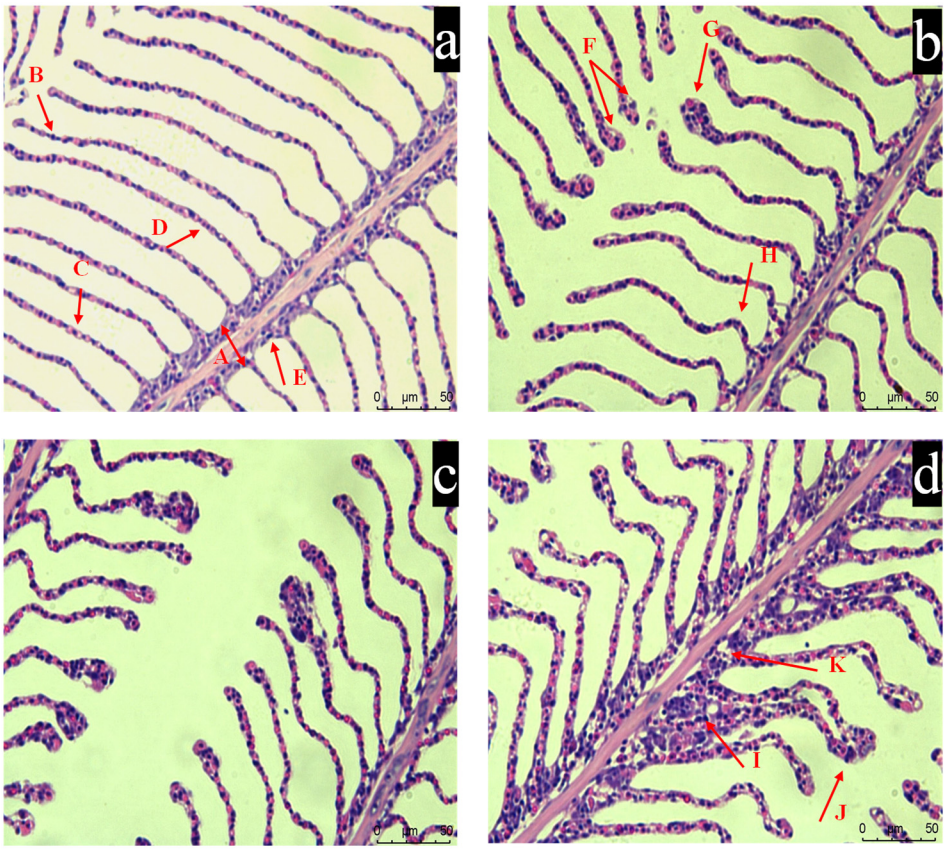

Figure 7. Impact of acute acidification stress on the histological structure of gills. (**a**): treatment group with pH 8.1 (control); (**b**): treatment group with pH 7.6; (**c**): treatment group with pH 7.1; and (**d**): treatment group with pH 6.6. (A): gill filaments; (B): gill lamella; (C): epithelial cells; (D): columnar cell; (E): chloride cells; (F): oedema of epithelial cells; (G): pestle hypertrophy of gill lamella; (H): gill lamella bend; (I): basal hyperplasia; (J): gill lamella adhered to each other; (K): cellular vacuoles.

Table 2. Semi-quantitative scoring of histopathological damage in gill tissues of yellowfin tuna juveniles under different pH treatments.

Group	pH 8.1	pH 7.6	pH 7.1	pH 6.6
Cellular edema	0	2	3	3
Cellular hyperplasia	0	2	3	4
Cellular adhesion	0	1	2	3
Cellular necrosis	0	1	3	3

Note: Three tissue samples were randomly selected from each treatment group, and 10 fields of view were randomly selected from each fish for observation. The severity of lesions was classified according to the number of affected cells per field of view as follows: 0 cells = Grade 0 (normal), 1–5 cells = Grade 1 (mild), 6–10 cells = Grade 2 (moderate), 11–15 cells = Grade 3 (severe), and >15 cells = Grade 4 (highly severe).

4. Discussion

4.1. Impact of Reduced pH on the Digestive Function of Yellowfin Tuna

Numerous studies have investigated the effects of environmental changes on digestive enzyme activities in marine species. For instance, prolonged darkness exposure was shown to suppress digestive enzyme secretion in juvenile European seabass (*Dicentrarchus labrax L.*) [45], while lead exposure at varying concentrations induced irregular fluctuations in digestive enzyme activities in 2-month-old (30–60 days post-hatching) Nile tilapia (*Oreochromis niloticus*) [46]. *Alosa sapidissima* [47] 1+ year-old subadult fish exhibited significantly reduced pepsin activity after 48 h at 30 °C. *Pampus argenteus* [48] showed a significant upward trend in both pepsin and trypsin activity with increasing stress duration at 32 °C over 48 h. Yellowfin tuna [49] exhibited increased trypsin activity with rising stress temperatures at 34 °C after 24 h. Juvenile cobia [50] (*Rachycentron canadum*) showed decreased MAS, LPS, and trypsin activities with reduced dissolved oxygen levels in hypoxic conditions.

Barramundi Lates calcarifer larvae [51] (*Lates calcarifer*) exhibited decreased protease activity under high ammonia nitrogen concentrations. These studies indicate that various environmental factors (temperature, light, heavy metals, ammonia nitrogen, etc.) exert markedly different effects on fish digestive enzyme activity. Such variations likely correlate with fish diet, digestive organs, and the duration and intensity of stress exposure. In the present study, pepsin activity showed an initial increase followed by a decrease, which differs to some extent from certain previous findings. When external environments acidify (e.g., seawater pH decreases from 8.1 to 7.6), potentially causing slight pH shifts within fish tissues (such as the stomach) or exposing them to acidification threats, organisms attempt to compensate for reduced efficiency of individual enzyme molecules due to pH increases by upregulating the gene expression and synthesis of pepsinogen. This represents a "quantity over quality" strategy. For example, studies on Chinese white shrimp (*Fenneropenaeus chinensis*) revealed that under low pH stress, shrimp maintain digestive function by increasing digestive enzyme gene expression and zymogen synthesis [52]. Although crustaceans were studied, this physiological adaptation strategy is widely applicable in fish. pH 7.6 may represent a "moderate stress" level sufficient to trigger the organism's strongest compensatory response. Furthermore, when exposed to highly acidic environments, fish typically exhibit a significant increase in water intake [53]. This may lead to excessive dilution of gastric fluids, thereby reducing gastric acid concentration and impairing digestive efficiency [54,55]. At even lower pH levels (7.1, 6.6), the stress becomes so severe that it may trigger energy reallocation (for coping with oxidative stress, ion regulation, etc.), which in turn inhibits the biosynthesis of digestive enzymes. Furthermore, the substantial intake of seawater may alter the concentration of inorganic ions in the fish digestive tract. These inorganic ions may act as activators or inhibitors of digestive enzymes, directly affecting the enzyme active sites to regulate digestive enzyme function, ultimately leading to different trends in enzyme activity changes [28]. Results indicate that pH 7.6 may represent a mild to moderate stress level sufficient to activate stress and compensatory mechanisms in yellowfin tuna juveniles.

The activity trend of trypsin was similar to that of pepsin, showing an increase followed by stabilization at pH 7.6. Comparable phenomena have been observed in Nile tilapia [46], juvenile American shad (*Alosa sapidissima*) [56], and juvenile European seabass [45]. These results suggest that under environmental stress, fish may enhance proteolytic capacity by elevating pyloric caeca protease activity to meet increased metabolic and stress resistance demands. Seawater acidification (reducing pH to 7.6) acts as a stressor that alters energy metabolism patterns in fish. The organism may require increased energy to regulate osmotic pressure and maintain acid-base balance (via energy-consuming ion pumps such as Na^+/K^+-ATPase). To meet this heightened energy demand, the organism may enhance digestive absorption capacity, thereby upregulating the synthesis of key proteases (e.g., trypsin). Studies on Atlantic salmon (*Salmo salar*) juveniles have revealed that moderate stress can stimulate growth and metabolic performance, a phenomenon termed the "hormetic effect" [57]. Journal of Experimental Biology). pH 7.6 may represent precisely such a "moderate stress" level for yellowfin tuna juveniles, triggering positive physiological responses. At more extreme pH values, however, this stimulatory effect disappears and is replaced by inhibition. However, the above conjecture requires further testing of the mRNA expression levels of pepsinogen and trypsinogen (e.g., via qPCR) to validate changes in synthesis at the transcriptional level.

The activities of hepatic digestive enzymes (amylase, AMS, and lipase, LPS) initially increased, followed by a decrease, along with a reduction in protease activity. This pattern suggests that fish may activate a compensatory mechanism to enhance carbohydrate and lipid digestion when protein digestive efficiency is compromised. Such metabolic switching could represent an adaptive strategy to maintain energy homeostasis under conditions of impaired protein digestion. However, the precise mechanism underlying this enzymatic compensation remains unresolved. Specifically, it remains to be determined whether the observed shifts in digestive enzyme profiles in tuna organs result from: (1) upregulation of the same enzymes or (2) induction of additional enzyme classes in response to acidic stress. Further investigation is required to elucidate these adaptive responses at the molecular level.

The activities of amylase (AMS) and lipase (LPS) in the foregut exhibited a decreasing trend, reaching their lowest levels at pH 7.1. Further reduction in pH may induce denaturation or inactivation of these enzymes, impairing their efficiency in carbohydrate and lipid breakdown. This observation underscores the critical importance of maintaining a stable internal pH for optimal enzymatic function. Consistent with our findings, previous studies have reported similar declines in AMS and LPS activities in mussels under acidified conditions [15,16]. It has been hypothesized that acidification exposure may alter the internal pH environment of digestive glands, leading to conformational changes, denaturation, or inactivation of digestive enzymes, ultimately causing structural damage to tissues. Furthermore, juvenile flounder exposed to combined stressors of elevated temperature and reduced pH also demonstrated significantly decreased AMS activity [58]. In environments where mussels face the combined effects of ocean acidification, hypoxia, and warming, both AMS and LPS activity decline [15]. Similar phenomena were observed in half-smooth tongue sole under high-density aquaculture conditions and in

European perch under different photoperiods [59]. These comprehensive findings indicate that when marine organisms face multiple environmental stresses—such as ocean warming, hypoxia, and acidification—similar response mechanisms may emerge. Collectively, these responses reflect how the failure of protective mechanisms can lead to overall physiological decline, ultimately impairing feeding and digestive functions. The current study further supports this conclusion, demonstrating that seawater acidification-induced suppression of digestive enzyme activities may disrupt key digestive processes, thereby compromising nutrient absorption capacity and growth potential in juvenile fish.

4.2. Effect of Low pH on the Metabolic Capacity of Yellowfin Tuna

Alanine aminotransferase (ALT) and aspartate aminotransferase (AST) are essential detoxification enzymes primarily located in fish hepatocytes and cardiomyocytes [60]. They play a vital role in maintaining whole-body energetic homeostasis and are considered sensitive biomarkers of fish health in response to stress, water contaminants, and disease [61]. Elevated ALT and AST activities often indicate liver injury, as their levels increase when the liver is damaged [62].

Fazio et al. [60] observed that in mullet (Mugil cephalus), liver AST and ALT activities increased with higher salinity, implying that the elevated enzyme levels reflected increased permeability and cellular leakage from hepatocytes. In a similar study, Vargas-Chacoff et al. [61] reported a marked rise in ALT levels in the liver of gilthead sea bream (*Sparus aurata*) with simultaneous increases in temperature and salinity, while hepatic AST activity decreased as salinity increased under constant temperature conditions. Large Yellow Croaker showed increased ALT and AST activities with increasing ammonia concentration under acute ammonia exposure conditions [62]. Epinephelus moara [63] exhibited a trend of initially decreasing followed by increasing ALT and AST activity after a sudden drop in salinity, whereas long-term nitrite exposure in Chinese perch [64] (*Siniperca chuatsi*) showed the opposite pattern for ALT and AST compared to Epinephelus moara. During adaptation to high temperatures in blue tilapia [65] (*Oreochromis aureus*), lactate dehydrogenase activity significantly increased in white muscle tissue, while liver lactate dehydrogenase activity showed an opposite trend. These findings indicate that enzyme activity changes in fish responding to environmental stress represent a dynamic, tissue-specific, and complex response reflecting their adaptive strategies and injury severity. In this study, the patterns of ALT and AST changes were generally similar; both were significantly higher at pH 7.6 compared to the control group, followed by a decline. These trends were similar to those observed in Asian seabass (*Lates calcarifer*) [66]. The initial increase in ALT and AST activity may be a response to mild stress caused by a change in pH, with the liver temporarily accelerating its metabolic processes in response to the altered conditions, leading to an increase in these enzymes to maintain homeostasis. However, highly acidic environments can disrupt normal metabolic processes in marine organisms, leading to oxidative stress [67]. Where the balance between the production of reactive oxygen species (ROS) and the body's ability to detoxify these reactive by-products or repair the resulting damage is disturbed. This oxidative stress may impair liver function and decrease the activity of liver enzymes such as ALT and AST [68]. This may explain the decrease in ALT and AST at pH 7.1 and 6.6. A similar initial increase followed by a decrease in both ALT and AST was observed in topmouth culter (*Erythroculter ilishaeformis*) exposed to nitrite [69], with comparable results also documented in yellowfin seabream (*Acanthopagrus latus*) and Asian seabass [66]. These fluctuations indicate intricate biological reactions to environmental stressors, emphasizing the delicate equilibrium that organisms strive to maintain in order to sustain physiological homeostasis under challenging conditions.

Lactate dehydrogenase (LDH) is crucial in converting lactate, a major by-product of anaerobic glycolysis, to pyruvate through oxidation in the presence of NADH [70]. Pyruvate kinase (PK) catalyzes the transformation of phosphoenolpyruvate to pyruvate, generating adenosine triphosphate (ATP), which is crucial for energy metabolism in tissues [71]. Prolonged adaptation to hypercapnia leads to significant changes in anaerobic metabolism indicators such as PK and LDH, with elevated activities of both indicating a shift from aerobic to anaerobic metabolism [72]. LDH and PK activities were consistently elevated in the hearts of Sparus aurata persistently exposed to a highly carbonated acidic environment (pH 7.3) [72], suggesting that continuous exposure to stressful conditions increases metabolic rate in response to environmental stressors, leading to elevated LDH levels [73]. In this study, LDH and PK activities were significantly higher in the pH 6.6-treated group than in the control group, indicating a stimulatory effect of the acidic environment on the glycolytic pathway. This increase suggests increased metabolic stress in fish, where glycolysis rates increase to provide energy to cope with the stress. A similar phenomenon was observed in the serum of juvenile Sagor catfish (*Hexanematichthys sagor*) [74] and in the liver of large yellow croaker [62], all showing elevated LDH activity under low pH conditions. This likely represents an enhanced metabolic response to acidification stress, resulting in increased lactate dehydrogenase levels [73]. Additionally, Nile tilapia exposed to

strongly alkaline conditions (pH 10.0) exhibited respiratory depression [75], where insufficient tissue oxygenation enhanced glycolysis, and excessive lactate accumulation ultimately induced acidosis, disrupting normal physiological functions—A mechanism sharing certain similarities with observations in the current study. Juvenile Pacific oysters (*Crassostrea gigas*) [76] exhibit significantly increased PK activity when exposed to environmental stress, a trend consistent with the PK activity changes observed in juvenile yellowfin tuna in the present study. This suggests that under changing environmental conditions, juvenile tuna may enhance PK activity to redistribute energy resources, thereby meeting increased energy demands during stress responses. However, the specific molecular pathways underlying this regulatory mechanism require further investigation and validation. Although PK plays a crucial role in glycolysis and energy metabolism, its activity varies across species under different environmental conditions, reflecting the complexity and species-specificity of metabolic regulation. Therefore, further research on PK activity regulation and its role in environmental adaptation is essential for a deeper understanding of the energy metabolism strategies employed by juvenile yellowfin tuna under acidification and other environmental stressors, as well as their implications for growth and survival.

Na^+K^+-ATPase (NKA) is a special protein present in the cell membrane of gill filaments, which consumes ATP in an active transport mode for Na^+ and K^+ ion exchange transport, providing the driving force for active transmembrane transport of ions against the concentration gradient, and is an important indicator of osmotic pressure regulation in fish [77]. Elevated NKA enzyme activity enhances cellular uptake of external inorganic ions, thereby maintaining stable ion levels inside and outside the cell and osmotic pressure balance [78]. Studies have shown that NKA enzymes in the gills of aquatic animals are sensitive to changes in seawater pH. For example, Atlantic salmon (*Salmo salar* L.) exhibited increased NKA activity in high-acid environments at different temperatures (5 °C and 15 °C) [79], and European sea bass showed similar changes in low pH environments over five weeks [53]. Juvenile Nile tilapia [75] displayed reduced NKA activity under extreme pH conditions, suggesting impaired Na+ influx capacity or diminished transepithelial transport efficiency, potentially due to pH-induced suppression of ATP metabolism across organs. These findings suggest that NKA activity in aquatic animals varies with water pH and may involve similar ionic regulatory mechanisms. In this study, NKA enzyme activity initially tended to increase with decreasing pH, consistent with the above findings. This suggests that the metabolic activity of juvenile tuna increases after acidification stress, requiring additional energy consumption to maintain osmotic pressure balance. NKA, as an energy enzyme, carries out cellular ion regulation and acid-base balance by consuming a large amount of cellular energy in the form of ATP. Therefore, an increase in NKA activity intensifies the consumption of cellular energy, reducing the ATP available for other processes. This suggests that fish may activate multiple physiological mechanisms under acidic stress to maintain metabolism and electrolyte homeostasis. However, the ion regulatory response of juvenile yellowfin tuna in low pH water still requires further study. These findings underscore the profound physiological impacts of environmental stressors on fish. Future studies should elucidate the molecular regulation of NKA activity and conduct systematic analyses integrating multiple physiological parameters to comprehensively assess acidification effects on osmoregulatory adaptations and associated survival risks.

4.3. The Effect of Low pH on the Histological Structure of Yellowfin Tuna

The use of histopathology of the digestive tract provides a suitable platform for assessing the health of fish, as most contaminants that enter the body will at some point enter the gut and alter the intestinal junctions [80]. The mucosal epithelium is distributed with a large number of goblet cells, which secrete digestive enzymes and other mucus. Digestive enzymes improve the efficiency of nutrient absorption, while other mucus lubricates the intestinal epithelium, playing a role in protecting the intestinal tract. Intestinal villi increase the surface area for absorption, significantly enhancing the digestive capacity and prolonging the retention time of chyme in the intestine. This facilitates the breakdown of nutrients by digestive enzymes and their subsequent absorption. The villi contain cells that secrete various digestive enzymes, including α-amylase, lipase, and protease, which aid in the breakdown of large molecules such as carbohydrates, fats, and proteins. These enzymes play a crucial role in nutrient absorption and contribute to improved growth performance [81]. The height and width of the intestinal villi are usually used as the main indicators for evaluating the functional state of the intestine. The larger the area of intestinal villi, the larger the absorptive area of the intestinal tract, and the better the digestive and absorptive capacity of the organism [82]. The midgut is primarily responsible for nutrient absorption, and a decrease in foregut digestive enzyme activity means that larger, undigested, or partially digested food particles will enter the midgut. Therefore, the midgut may undergo structural changes to adapt to the altered digestive environment. In the present study, the midgut intestinal villi of the pH 7.1 treatment group were bent and shortened in height from the onset of histological observation, and the phenomenon tended to worsen with increasing acidity. Suggesting that low pH

water affects the digestive function of yellowfin tuna, midgut epithelial cells exhibit hypertrophy (increase in cell size) or hyperplasia (increase in cell number) as a compensatory mechanism to enhance the absorptive surface area in an attempt to absorb more nutrients from poorly digested food. Yellowtail kingfish [83] (*Seriola lalandi*) and Atlantic cod [40] also exhibited similar results in low-pH environments.

The gills of fish are in direct contact with the water environment, allowing them to sense changes in water acidity quickly, leading to various cell changes in the gills. Changes in the epidermal cells of gill filaments are particularly crucial for the physiological function of gills. Environmental stress can cause two main types of damage to fish gills: direct damage such as cell death and detachment, and defensive damage such as thickening and enlargement of gill lamellae and proliferation of epithelial cells [84]. Under environmental stress, Chinese perch (*Siniperca chuatsi*) [64] and juvenile blunt snout bream (*Megalobrama amblycephala*) [85] have shown both direct and defensive damage responses, such as oedema, fusion, and hyperplasia of gill lamellae. In this study, oedema appeared in the epithelial cells of gill filaments at pH 7.6, increased at pH 6.6, and hyperplasia appeared at the base, similar to the results of the above studies. This may be due to impaired cellular function, affecting the function of sodium-potassium pumps on the cell membrane. This results in the accumulation of solutes and other substances in the epithelial cells, leading to water osmotic influx [86]. The pH 6.6 treatment group showed a rapid increase in NKA enzyme activity, indicating increased energy expenditure. As pH decreased, gills began to show irreversible damage such as epithelial rupture and detachment, cellular vacuolization, and basal cell vacuolisation of gill lamellae. This suggests that persistent acidity stress can disrupt the structural integrity of gills, impairing their respiratory function.

5. Conclusions

This study examined the impact of acute acidification on digestive enzyme activities, metabolic enzyme functions, and tissue morphology in juvenile yellowfin tuna. The results demonstrated that digestive enzymes maintained normal function at pH 7.6. However, when seawater pH drops to 6.6, gill lamellae proliferate and adhere, digestive enzyme activity in the gut decreases linearly, and tissue structure is damaged, impairing digestive function. These findings further elucidate the mechanisms underlying juvenile yellowfin tuna's response to acidification stress, providing reference data for future net-pen aquaculture of this species in challenging coastal environments, thereby indirectly guiding the development of aquaculture practices.

Supplementary Materials

The additional data and information can be downloaded at: https://media.sciltp.com/articles/others/250911111700 8951/ALE-2508000311-Supplementary-Materials.pdf. Table S1: Regression coefficients of trypsin activity. Table S2: Regression coefficients of pepsin activity.

Author Contributions

X.W. and Z.F.: Conceptualization; X.W., X.L. and J.B.: Methodology; Z.F. and J.B.: Software; X.L. and J.B.: Validation; X.W. and Z.F.: Formal Analysis; X.W. and Z.F.: Investigation; J.B.: Resources; X.W. and X.L.: Data Curation; X.W.: Writing—Original Draft; X.L., Z.F. and Z.M.: Writing—Review and Editing; X.W. and Z.F.: Visualization; Z.M.: Supervision; J.B.: Project Administration; Z.M.: Funding Acquisition. All authors have read and agreed to the published version of the manuscript.

Funding

This work was supported by the National Natural Science Foundation of China (32460927); the Central Fund for Guiding Local Science and Technology Development (guike ZY22096005); the Guangxi Science and Technology Planning Project (guike AD21238026); the Science and Technology special fund of Hainan Province (ZDYF2024XDNY247); the Central Public-interest Scientific Institution Basal Research Fund, CAFS (2025XT03, 2023TD58); the Project of Sanya Yazhou Bay Science and Technology City (SKJC-2022-PTDX-015).

Institutional Review Board Statement

The animal study was reviewed and approved by the Animal Care and Use Committee of the South China Sea Fisheries Research Institute, Chinese Academy of Fishery Sciences. The ethical code is 2020TD55, which was approved on 5 January 2020.

Informed Consent Statement

Not applicable.

Data Availability Statement

The data supporting the results of this study can be obtained from the corresponding author upon reasonable request.

Conflicts of Interest

The authors declare no conflict of interest.

Use of AI and AI-assisted Technologies

No AI tools were utilized for this paper.

References

1. Qin, J.; Ma, Z.; Li, Y. Review and Outlook for Research and Development in Aquatic Life and Ecosystems. *Aquat. Life Ecosyst.* **2015**, *1*, 2.
2. Orr, J.C.; Fabry, V.J.; Aumont, O.; et al. Anthropogenic ocean acidification over the twenty-first century and its impact on calcifying organisms. *Nature* **2005**, *437*, 681–686. https://doi.org/10.1038/nature04095.
3. Tang, Q.; Chen, C.T.; Yu, K.F.; et al. The effects of ocean acidification on marine organisms and ecosystem. *Chin. Sci. Bull.* **2013**, *58*, 1307–1314. https://doi.org/10.1360/972012-1596.
4. Mingle, J. *Special Report on the Ocean and Cryosphere in a Changing Climate*; IPCC: Geneva, Switzerland, 2020; Volume 67, pp. 49–51.
5. Glaspie, C.N.; Longmire, K.; Seitz, R.D. Acidification alters predator-prey interactions of blue crab Callinectes sapidus and soft-shell clam Mya arenaria. *J. Exp. Mar. Biol. Ecol.* **2017**, *489*, 58–65. https://doi.org/10.1016/j.jembe.2016.11.010.
6. Miller, S.H.; Breitburg, D.L.; Burrell, R.B.; et al. Acidification increases sensitivity to hypoxia in important forage fishes. *Mar. Ecol. Prog. Ser.* **2016**, *549*, 1–8. https://doi.org/10.3354/meps11695.
7. Robbins, L.L.; Lisle, J. Regional Acidification Trends in Florida Shellfish Estuaries: A 20+ Year Look at pH, Oxygen, Temperature, and Salinity. *Estuaries Coasts* **2018**, *41*, 1268–1281. https://doi.org/10.1007/s12237-017-0353-8.
8. Pörtner, H. Ecosystem effects of ocean acidification in times of ocean warming: A physiologist's view. *Mar. Ecol. Prog. Ser.* **2008**, *373*, 203–218. https://doi.org/10.3354/meps07768.
9. Enzor, L.A.; Hunter, E.M.; Place, S.P. The effects of elevated temperature and ocean acidification on the metabolic pathways of notothenioid fish. *Conserv. Physiol.* **2017**, *5*, cox019. https://doi.org/10.1093/conphys/cox019.
10. Melzner, F.; Göbel, S.; Langenbuch, M.; et al. Swimming performance in Atlantic Cod (*Gadus morhua*) following long-term (4–12 months) acclimation to elevated seawater P_{CO2}. *Aquat. Toxicol.* **2008**, *92*, 30–37. https://doi.org/10.1016/j.aquatox.2008.12.011.
11. Strobel, A.; Graeve, M.; Poertner, H.O.; et al. Mitochondrial acclimation capacities to ocean warming and acidification are limited in the antarctic *Nototheniid Fish*, *Notothenia rossii* and *Lepidonotothen squamifrons*. *PLoS ONE* **2013**, *8*, e68865. https://doi.org/10.1371/journal.pone.0068865.
12. Sokolova, M.I.; Frederich, M.; Bagwe, R.; et al. Energy homeostasis as an integrative tool for assessing limits of environmental stress tolerance in aquatic invertebrates. *Mar. Environ. Res.* **2012**, *79*, 1–15. https://doi.org/10.1016/j.|marenvres.2012.04.003.
13. Louise, C.; Marta, M.; Guy, C.; et al. Food availability modulates the combined effects of ocean acidification and warming on fish growth. *Sci. Rep.* **2020**, *10*, 2338. https://doi.org/10.1038/s41598-020-58846-2.
14. Freitas, R.; Marchi, D.L.; Bastos, M.; et al. Effects of seawater acidification and salinity alterations on metabolic, osmoregulation and oxidative stress markers in *Mytilus galloprovincialis*. *Ecol. Indic.* **2017**, *79*, 54–62. https://doi.org/10.1016/j.ecolind.2017.04.003.
15. Khan, F.U.; Hu, M.; Kong, H.; et al. Ocean acidification, hypoxia and warming impair digestive parameters of marine mussels. *Chemosphere* **2020**, *256*, 127096. https://doi.org/10.1016/j.chemosphere.2020.127096.
16. Xu, M.; Sun, T.; Tang, X.; et al. Title: CO_2 and HCl-induced seawater acidification impair the ingestion and digestion of blue mussel *Mytilus edulis*. *Chemosphere* **2020**, *240*, 124821. https://doi.org/10.1016/j.chemosphere.2019.124821.
17. Hancock, J.R.; Place, S.P. Impact of ocean acidification on the hypoxia tolerance of the woolly sculpin, *Clinocottus analis*. *Conserv. Physiol.* **2016**, *4*, w40. https://doi.org/10.1093/conphys/cow040.
18. Xu, Z.; Zhang, H.; Guo, M.; et al. Analysis of Acute Nitrite Exposure on Physiological Stress Response, Oxidative Stress, Gill Tissue Morphology and Immune Response of Large Yellow Croaker (*Larimichthys crocea*). *Animals* **2022**, *12*, 1791. https://doi.org/10.3390/ANI12141791.

19. Fivelstad, S.; Waagbø, R.; Zeitz, S.F.; et al. A major water quality problem in smolt farms: Combined effects of carbon dioxide, reduced pH and aluminium on Atlantic salmon (*Salmo salar* L.) smolts: Physiology and growth. *Aquaculture* **2003**, *215*, 339–357. https://doi.org/10.1016/S0044-8486(02)00197-7.
20. Schmidt, M.; Gerber, R.; Fielder, D.S. Effects of ocean acidification on digestive enzymes and intestinal morphology in a marine fish. *Mar. Biol.* **2019**, *166*, 151.
21. Frommel, Y.A.; Maneja, R.; Lowe, D.; et al. Severe tissue damage in Atlantic cod larvae under increasing ocean acidification. *Nat. Clim. Chang.* **2012**, *2*, 42–46.
22. Frommel, A.Y.; Maneja, R.; Lowe, D.; et al. Organ damage in Atlantic herring larvae as a result of ocean acidification. *Ecol. Appl.* **2014**, *24*, 1131–1143.
23. Ilyina, T.; Six, K.D.; Segschneider, J.; et al. Global ocean biogeochemistry model HAMOCC: Model architecture and performance as component of the MPI-Earth system model in different CMIP5 experimental realizations. *J. Adv. Model. EarthSyst.* **2013**, *5*, 287–315. https://doi.org/10.1029/2012MS000178.
24. Feely, R.A.; Sabine, C.L.; Hernandez-Ayon, J.M.; et al. Evidence for Upwelling of Corrosive "Acidified" Water onto the Continental Shelf. *Science* **2008**, *320*, 1490–1492. https://doi.org/10.1126/science.1155676.
25. Manzello, D.P. Ocean acidification hotspots: Spatiotemporal dynamics of the seawater CO_2 system of eastern Pacific coral reefs. *Limnol. Oceanogr.* **2010**, *55*, 239–248. https://doi.org/10.4319/lo.2010.55.1.0239.
26. Frommel, Y.A.; Margulies, D.; Wexler, B.J.; et al. Ocean acidification has lethal and sub-lethal effects on larval development of yellowfin tuna, *Thunnus albacares*. *J. Exp. Mar. Biol.Ecol.* **2016**, *482*, 18–24.
27. Bromhead, D.; Scholey, V.; Nicol, S.; et al. The potential impact of ocean acidification upon eggs and larvae of yellowfin tuna (*Thunnus albacares*). *Deep. Sea Res. Part II Top. Stud. Oceanogr.* **2015**, *113*, 268–279.
28. Shengjie, Z.; Ninglu, Z.; Zhengyi, F.; et al. Impact of Salinity Changes on the Antioxidation of Juvenile Yellowfin Tuna (*Thunnus albacares*). *J. Mar. Sci. Eng.* **2023**, *11*, 132. https://doi.org/10.3390/jmse11010132.
29. Havice, E. The structure of tuna access agreements in the Western and Central Pacific Ocean: Lessons for Vessel Day Scheme planning. *Mar. Policy* **2010**, *34*, 979–987. https://doi.org/10.1016/j.marpol.2010.02.004.
30. Bell, D.J.; Ganachaud, A.; Gehrke, C.P.; et al. Mixed responses of tropical Pacific fisheries and aquaculture to climate change. *Nat. Clim. Chang.* **2013**, *3*, 591–599. https://doi.org/10.1038/nclimate1838.
31. Juan-Jordá, M.J.; Mosqueira, I.; Cooper, A.B.; et al. Global population trajectories of tunas and their relatives. *Proc. Natl. Acad. Sci. USA* **2011**, *108*, 20650–20655. https://doi.org/10.1073/pnas.1107743108.
32. Inter-American Tropical Tuna Commission. *Tunas and Billfishes in the Eastern Pacific Ocean in 2006*; Inter-American Tropical Tuna Commission (IATTC): La Jolla, CA, USA, 2008; pp. 10–100.
33. Fu, Z.; Bai, J.; Ma, Z. Physiological Adaptations and Stress Responses of Juvenile Yellowfin Tuna (*Thunnus albacares*) in Aquaculture: An Integrative Review. *Aquat. Life Ecosyst.* **2025**, *1*, 3.
34. Wexler, B.J.; Scholey, P.V.; Olson, J.R.; et al. Tank culture of yellowfin tuna, *Thunnus albacares*: Developing a spawning population for research purposes. *Aquaculture* **2003**, *220*, 327–353.
35. Fu, Z.; Qin, J.G.; Ma, Z.; et al. Acute acidification stress weakens the head kidney immune function of juvenile Lates calcarifer. *Ecotoxicol. Environ. Saf.* **2021**, *225*, 112712. https://doi.org/10.1016/J.ECOENV.2021.112712.
36. Caldeira, K.; Wickett, M.E. Anthropogenic carbon and ocean pH. *Nature* **2003**, *425*, 365. https://doi.org/10.1038/425365a.
37. Ilyina, T.; Zeebe, R.E.; Reimer, E.M.; et al. Early detection of ocean acidification effects on marine calcification. *Glob. Biogeochem. Cycles* **2009**, *23*, B1008–B1011. https://doi.org/10.1029/2008GB003278.
38. Shi, W.; Zhao, X.; Han, Y.; et al. Effects of reduced pH and elevated pCO_2 on sperm motility and fertilisation success in blood clam, *Tegillarca granosa*. *N. Z. J. Mar. Freshwater Res.* **2017**, *51*, 543–554. https://doi.org/10.1080/00288330.2017.1296006.
39. Ohno, Y.; Iguchi, A.; Shinzato, C.; et al. An aposymbiotic primary coral polyp counteracts acidification by active pH regulation. *Sci. Rep.* **2017**, *7*, 40324. https://doi.org/10.1038/SREP40324.
40. Sun, T.; Tang, X.; Zhou, B.; et al. Comparative studies on the effects of seawater acidification caused by CO_2 and HCl enrichment on physiological changes in Mytilus edulis. *Chemosphere* **2016**, *144*, 2368–2376. https://doi.org/10.1016/j.chemosphere.2015.10.117.
41. Rosseland, B.O.; Massabuau, J.C.; Grimalt, J.; et al. Fish ecotoxicology: European mountain lake ecosystems regionalisation, diagnostic and socio-economic evaluation (EMERGE). In *Fish Sampling Manual for Live Fish*; Norwegian Institute for Water Research (NIVA): Oslo, Norway, 2003; p. 23.
42. Gonçalves, M.; Lopes, C.; Silva, P. Comparative histological description of the intestine in platyfish (*Xiphophorus maculatus*) and swordtail fish (*Xiphophorus helleri*). *Tissue Cell* **2024**, *87*, 102306. https://doi.org/10.1016/J.TICE.2024.102306.
43. Cui, Y.; Lin, X.D.; Kang, M.L.; et al. Low temperature combined with high-humidity thawing reduced the physicochemical quality deterioration of Pampus argenteus. *Mod. Food Sci. Technol.* **2018**, *34*, 81–89. https://doi.org/10.13982/j.mfst.1673-9078.2018.8.013.

44. Huang, J.; Fu, Z.; Bai, J.; et al. Cold stress disrupts gill homeostasis in juvenile yellowfin tuna (*Thunnus albacares*) by altering oxidative, metabolic, and immune responses. *Mar. Environ. Res.* **2025**, *210*, 107300. https://doi.org/10.1016/J.MARENVRES.2025.107300.
45. Li, X.; Wei, P.; Liu, S.; et al. Photoperiods affect growth, food intake and physiological metabolism of juvenile European Sea Bass (*Dicentrachus labrax* L.). *Aquac. Rep.* **2021**, *20*, 100656. https://doi.org/10.1016/J.AQREP.2021.100656.
46. Álvarez-González, A.C.; Martínez-Sánchez, L.; Peña-Marín, S.E.; et al. Effects on the Growth and Digestive Enzyme Activity in Nile Tilapia Fry (*Oreochromis niloticus*) by Lead Exposure. *Water Air Soil Pollut.* **2020**, *231*, 197–206. https://doi.org/10.1007/s11270-020-04810-9.
47. Yang, M.; Jiang, F.; Shi, Y.; et al. Effect of high temperature stress on activities of digestive enzymes in *Alosa sapidissima*. *J. Northwest A F Univ.* **2020**, *48*, 1–8.
48. Shi, Z.H.; Xie, M.M.; Peng, S.M.; et al. Effects of Temperature Stress on Activities of Digestive Enzymes and Serum Biochemical Indices of *Pampus argenteus* Juveniles. *Prog. Fish. Sci.* **2016**, *37*, 30–37.
49. Liu, H.Y.; Yang, R.; Fu, Z.Y.; et al. Acute thermal stress increased enzyme activity and muscle energy distribution of yellowfin tuna. *PLoS ONE* **2023**, *18*, e0289606.
50. Yang, E.J.; Zhang, J.D.; Yang, L.T.; et al. Effects of hypoxia stress on digestive enzyme activities, intestinal structure and the expression of tight junction proteins coding genes in juvenile cobia (*Rachycentron canadum*). *Aquac. Res.* **2021**, *52*, 5630–5641.
51. Liu, Y.; Hu, J.; Zhou, S.; et al. Effect of acute ammonia stress on antioxidant enzymes and digestive enzymes in barramundi *Lates calcarifer* larvae. *Isr. J. Aquac. Bamidgeh* **2018**, *70*, 1508.
52. Liu, H.; Li, H.; Wei, H.; et al. Effects of low pH on the gene expression and activity of digestive enzymes in the giant freshwater prawn *Macrobrachium rosenbergii*. *Aquac. Res.* **2016**, *47*, 2779–2789.
53. Alves, A.; Gregório, F.S.; Ruiz-Jarabo, I.; et al. Intestinal response to ocean acidification in the European sea bass (*Dicentrarchus labrax*). *Comp. Biochem. Physiol. Part A Mol. Integr. Physiol.* **2020**, *250*, 110789. https://doi.org/10.1016/j.cbpa.2020.110789.
54. Noda, M.; Murakami, K. Studies on proteinases from the digestive organs of sardine. II. Purification and characterization of two acid proteinases from the stomach. *Biochim. Biophys. Acta* **1981**, *658*, 27–34. https://doi.org/10.1016/0005-2744(81)90246-1.
55. Kihara, M. Pepsin-like protease activity and the gastric digestion within ex vivo Pacific bluefin tuna Thunnus orientalis stomachs, as a gastric digestion model. *Anim. Feed. Sci. Technol.* **2015**, *206*, 87–99. https://doi.org/10.1016/j.anifeedsci.2015.05.009.
56. Liu, Z.F.; Gao, X.Q.; Yu, J.X.; et al. Effects of different salinities on growth performance, survival, digestive enzyme activity, immune response, and muscle fatty acid composition in juvenile American shad (*Alosa sapidissima*). *Fish Physiol. Biochem.* **2017**, *43*, 761–773. https://doi.org/10.1007/s10695-016-0330-3.
57. Anttila, K.; Lewis, M.; Prokkola, J.M.; et al. Warm acclimation and oxygen depletion induce species-specific responses in salmonids. *J. Exp. Biol.* **2015**, *218*, 1471–1477.
58. Pimentel, M.S.; Filipa, F.; Mário, D.; et al. Oxidative Stress and Digestive Enzyme Activity of Flatfish Larvae in a Changing Ocean. *PLoS ONE* **2015**, *10*, e134082. https://doi.org/10.1371/journal.pone.0134082.
59. Liu, G.; Ye, Z.; Liu, D.; et al. Influence of Stocking Density on Growth, Digestive Enzyme Activity, Immunity, and Cortisol Levels of Subadult Half-smooth Tongue Sole *Cynoglossus semilaevis* in a Recirculating Aquaculture System. *North Am. J. Aquac.* **2018**, *80*, 286–293.
60. Fazio, F.; Marafioti, S.; Arfuso, F.; et al. Influence of different salinity on haematological and biochemical parameters of the widely cultured mullet, *Mugil cephalus*. *Mar. Freshw. Behav. Physiol.* **2013**, *46*, 211–218. https://doi.org/10.1080/10236244.2013.817728.
61. Vargas-Chacoff, L.; Arjona, J.F.; Polakof, S.; et al. Interactive effects of environmental salinity and temperature on metabolic responses of gilthead sea bream *Sparus aurata*. *Comp. Biochem. Physiol. A Mol. Integr. Physiol.* **2009**, *154*, 417–424. https://doi.org/10.1016/j.cbpa.2009.07.015.
62. Guo, M.; Xu, Z.; Zhang, H.; et al. The Effects of Acute Exposure to Ammonia on Oxidative Stress, Hematological Parameters, Flesh Quality, and Gill Morphological Changes of the Large Yellow Croaker (*Larimichthys crocea*). *Animals* **2023**, *13*, 2534. https://doi.org/10.3390/ANI13152534.
63. Shi, Z.H.; Liao, L.Y.; Wang, X.S.; et al. Impact of abrupt salinity decrease on metabolic enzymes in the liver of *Epinehelus moara*. *Mar. Fish.* **2016**, *38*, 64–71.
64. Yanpeng, Z.; Fang, X.L.; Shan, H.; et al. Effects of long-term low-concentration nitrite exposure and detoxification on growth performance, antioxidant capacities, and immune responses in Chinese perch (*Siniperca chuatsi*). *Aquaculture* **2021**, *533*, 637123. https://doi.org/10.1016/j.aquaculture.2020.736123.
65. Younis, E.M. Variation in metabolic enzymatic activity in white muscle and liverof blue tilapia, Oreochromis aureus, in response to long-term thermalacc limatization. *Chin. J. Oceanol. Limnol.* **2015**, *33*, 696–704.

66. Torfi, M.M.; Omid, S.; Rahim, O.; et al. The effect of salinity on growth performance, digestive and antioxidant enzymes, humoral immunity and stress indices in two euryhaline fish species: Yellowfin seabream (*Acanthopagrus latus*) and Asian seabass (*Lates calcarifer*). *Aquaculture* **2021**, *534*, 736329. https://doi.org/10.1016/J.AQUACULTURE.2020.736329.
67. Heuer, R.M.; Grosell, M. Physiological impacts of elevated carbon dioxide and ocean acidification on fish. *Am. J. Physiol. Regul. Integr. Comp.Physiol.* **2014**, *307*, 1061–1084.
68. Zhang, J.; Li, X.; Zhao, C.; et al. The role of oxidative stress in liver injury and the protective effects of antioxidant agents in aquatic animals. *Aquat. Toxicol.* **2023**, *264*, 106730. https://doi.org/10.1016/j.aquatox.2023.106730.
69. Eggestøl, H.Ø.; Lunde, H.S.; Haugland, G.T. The proinflammatory cytokines TNF-α and IL-6 in lumpfish (*Cyclopterus lumpus* L.)-identification, molecular characterization, phylogeny and gene expression analyses. *Dev. Comp. Immunol.* **2020**, *105*, 103608.
70. Powers, D.A.; Lauerman, T.; Crawford, D.; et al. Genetic mechanisms for adapting to a changing environment. *Annu. Rev. Genet.* **1991**, *25*, 629–660. https://doi.org/10.1146/annurev.ge.25.120191.003213.
71. Jia, Y.; Jing, Q.; Xing, Z.; et al. Effects of two different culture systems on the growth performance and physiological metabolism of tiger pufferfish (*Takifugu rubripes*). *Aquaculture* **2018**, *495*, 267–272. https://doi.org/10.1016/j.aquaculture.2018.05.049.
72. Michaelidis, B.; Spring, A.; Pörtner, O.H. Effects of long-term acclimation to environmental hypercapnia on extracellular acid–base status and metabolic capacity in Mediterranean fish *Sparus aurata*. *Mar. Biol.* **2007**, *150*, 1417–1429. https://doi.org/10.1007/s00227-006-0436-8.
73. Ming-Jian, L.; Hua-Yang, G.; Bo, L.; et al. Gill oxidative damage caused by acute ammonia stress was reduced through the HIF-1α/NF-κb signaling pathway in golden pompano (*Trachinotus ovatus*). *Ecotoxicol. Environ. Saf.* **2021**, *222*, 112504. https://doi.org/10.1016/J.ECOENV.2021.112504.
74. Noor, N.M.; De, M.; Cob, Z.C.; et al. Welfare of scaleless fish, Sagor catfish (*Hexanematichthys sagor*) juveniles under different carbon dioxide concentrations. *Aquac. Res.* **2021**, *52*, 2980–2987.
75. Qiang, J.; Wang, H.; Li, R.W.; et al. Effects of acid and alkaline stress on energy metabolism of *Oreochromis niloticus* juveniles with different body mass. *Chin. J. Appl. Ecol.* **2011**, *22*, 2438–2446.
76. Epelboin, Y.; Quere, C.; Pernet, F.; et al. Energy and antioxidant responses of pacific oyster exposed to trace levels of pesticides. *Chem. Res. Toxicol.* **2015**, *28*, 1831–1841. https://doi.org/10.1021/acs.chemrestox.5b00269
77. Hirose, S.; Kaneko, T.; Naito, N.; et al. Molecular biology of major components of chloride cells. *Comp. Biochem. Physiol. B Biochem. Mol. Biol.* **2003**, *136*, 593–620. https://doi.org/10.1016/S1096-4959(03)00287-2.
78. De Weer, P.; Gadsby, D.C.; Rakowski, R.F. Voltage dependence of the apparent affinity for external Na(+) of the backward-running sodium pump. *J. Gen. Physiol.* **2001**, *117*, 315–328. https://doi.org/10.1085/jgp.117.4.315.
79. Fivelstad, S.; Waagbø, R.; Stefansson, S.; et al. Impacts of elevated water carbon dioxide partial pressure at two temperatures on Atlantic salmon (*Salmo salar* L.) parr growth and haematology. *Aquaculture* **2007**, *269*, 241–249. https://doi.org/10.1016/j.aquaculture.2007.05.039.
80. Filippov, A.A.; Golovanova, L.I.; Aminov, I.A. Effects of organic pollutants on fish digestive enzymes: A review. *Inland Water Biol.* **2013**, *6*, 155–160. https://doi.org/10.1134/S199508291302003X.
81. Yang, J.; Zhou, S.; Fu, Z.; et al. Fermented Astragalus membranaceus could promote the liver and intestinal health of juvenile tiger grouper (*Epinephelus fuscoguttatus*). *Front. Physiol.* **2023**, *14*, 1264208. https://doi.org/10.3389/FPHYS.2023.1264208.
82. Zhang, N.; Yang, R.; Fu, Z.; et al. Mechanisms of Digestive Enzyme Response to Acute Salinity Stress in Juvenile Yellowfin Tuna (*Thunnus albacares*). *Animals* 2023. 13, 3534. https://doi.org/10.3390/ANI13223454.
83. Frommel, A.Y.; Brauner, C.J.; Allan BJ, M.; et al. Organ health and development in larval kingfish are unaffected by ocean acidification and warming. *PeerJ* **2019**, *7*, e8266.
84. Fanta, E.; Rios, S.F.; Romão, S.; et al. Histopathology of the fish *Corydoras paleatus* contaminated with sublethal levels of organophosphorus in water and food. *Ecotoxicol. Environ. Saf.* **2003**, *54*, 119–130. https://doi.org/10.1016/S0147-6513(02)00044-1.
85. Zhang, W.; Sun, S.; Ge, X.; et al. Acute effects of ammonia exposure on the plasma and haematological parameters and histological structure of the juvenile blunt snout bream, *Megalobrama amblycephala*, and post-exposure recovery. *Aquac.Res.* **2018**, *2*, 1008–1019. https://doi.org/10.1111/are.13548.
86. Huang, C.; Feng, L.; Liu, X.; et al. The toxic effects and potential mechanisms of deoxynivalenol on the structural integrity of fish gill: Oxidative damage, apoptosis and tight junctions disruption. *Toxicon* **2019**, *174*, 32–42. https://doi.org/10.1016/j.toxicon.2019.12.151.